



CHORUS

This is the accepted manuscript made available via CHORUS. The article has been published as:

Microscopic Theory of Entangled Polymer Melt Dynamics: Flexible Chains as Primitive-Path Random Walks and Supercoarse Grained Needles

Daniel M. Sussman and Kenneth S. Schweizer

Phys. Rev. Lett. **109**, 168306 — Published 19 October 2012

DOI: [10.1103/PhysRevLett.109.168306](https://doi.org/10.1103/PhysRevLett.109.168306)

Microscopic Theory of Entangled Polymer Melt Dynamics: Flexible Chains as Primitive-Path Random Walks and Super Coarse-Grained Needles

Daniel M. Sussman^{1,+} and Kenneth S. Schweizer^{2,3*}

¹Department of Physics, ²Departments of Materials Science and Chemistry, and ³Frederick Seitz Materials Research Laboratory, University of Illinois, 1304 W. Green Street, Urbana, IL 61801

[*kschweiz@illinois.edu](mailto:kschweiz@illinois.edu)

+ present address: Department of Physics and Astronomy, University of Pennsylvania

PACS numbers: 47.57.Ng, 83.10.Kn

Abstract

We qualitatively extend a microscopic dynamical theory for the transverse confinement of infinitely thin rigid rods to study topologically entangled melts of flexible polymer chains. Our main result treats coils as ideal random walks of self-consistently determined primitive-path (PP) steps and exactly includes chain uncrossability at the binary collision level. A strongly anharmonic confinement potential (“tube”) for a primitive path is derived and favorably compared with simulation results. The relationship of the PP-level theory to two simpler models, the melt as a disconnected fluid of primitive-path steps, and a “super coarse-graining” that replaces the entire chain by a needle corresponding to its end-to-end vector, is examined. Remarkable connections between the different levels of coarse graining are established.

Understanding the fascinating and complex dynamics of concentrated liquids of large flexible polymer coils has been an ongoing challenge spanning many decades. From the point of view of simulations the vast range of length- and time-scales associated with dense melts or solutions of long chains poses a formidable challenge to studying the long-time dynamics [1]. The theoretical difficulty is that the topological constraints arising from chain connectivity and uncrossability (“entanglements”) dominate intermediate and long-time elasticity, relaxation, and transport when polymers become sufficiently long and/or concentrated. These singular interactions, combined with the statistical nature of polymer conformations, render a first-principles theory exceptionally challenging to formulate.

Since its introduction, the phenomenological reptation-tube model of deGennes, Doi, and Edwards [2, 3] has been the most common starting point for theoretical analysis. This single-chain approach postulates transverse localization beyond a mesoscopic length scale, the tube diameter d_T , as the dynamical consequence of the many interpenetrating chains on tagged polymer motion. The tube constraints are modeled by an infinitely strong (e.g., harmonic) confinement field, implying long-time diffusion proceeds only via anisotropic curvilinear motion. The reptation-tube theory and its diverse elaborations [4] are able to account for a remarkably broad class of experimental data, but it has recently been emphasized that the theory’s phenomenological nature can be a weakness, especially when evaluating proposed modifications to the model [5]. Particularly desirable is a theoretical explanation of the emergence of the localizing tube, the full spatially-resolved dynamic confinement potential, and the critical chain length that controls the crossover from unentangled to entangled behavior, N_e [5, 6].

In this Letter we adopt the classic Doi-Edwards (DE) picture of a polymer melt by coarse graining out the chain degrees of freedom on length scales smaller than some entanglement length L_e [3], but where we *microscopically* and *self-consistently* determine this length scale. A chain of N segments is mapped to an ideal random walk of $Z \equiv N / N_e$ “primitive path” (PP) steps of length $L_e = \sigma \sqrt{N_e}$, where σ is the statistical segment length such that $\langle R_{ee} \rangle = \sigma \sqrt{N}$ is the mean polymer end-to-end distance. This physical picture has been extensively used in simulation studies of the confining tube, where each chain is represented by rod-like PP segments, and topological entanglements correspond to the intersection of these rod-like segments [7, 8]. By qualitatively generalizing our theory for the dynamics of entangled rigid needles [9] to treat the topological interchain PP interactions, we construct a microscopic theory for the full tube confinement potential acting at the PP level. We also address long-time center of mass (CM) diffusion and end-to-end vector relaxation. Intriguingly, we find that the results from studying chains at the level of interacting PP steps are very similar to a “super coarse-graining” procedure [1] that replaces the entire coil with an uncrossable needle corresponding to R_{ee} .

We first consider the transverse confinement of the PP segment α on a tagged polymer in a melt with chain number density ρ , schematically depicted in Fig. 1. Transverse localization of segment α is initially treated as a Gaussian distribution with a mean characteristic length (“tube radius”) \bar{r}_l by self-consistently computing the long-time (localizing) part of the force-force time correlation function associated with a tagged segment interacting with the PP steps of another chain. Generalizing the dynamic mean-field theory of Szamel for non-rotating needles

[10, 11], the formal expression for this localization length under quenched-reptation conditions (i.e., holding chain ends fixed) is:

$$\frac{4}{\bar{r}_l^2} = \frac{-\rho}{16\pi^2} (\vec{I} - \vec{u}_\alpha \vec{u}_\alpha) : \sum_{j,k=1}^Z \int d\vec{v} d\gamma d\vec{r}_{\alpha 2} \vec{T}(\alpha j) (\Omega_{loc}^\dagger)^{-1} \vec{T}(\alpha k). \quad (1)$$

Here \vec{u}_i is the orientation of the PP step i , \vec{v} and γ describe the body-frame orientation of an instantaneous conformation of a second chain, $\vec{r}_{\alpha 2}$ is the CM separation between α and the second chain, and the colon denotes a double contraction of tensorial indices. The collision operator $\vec{T}(\alpha j)$ encodes effective forces at the level of impulsive interactions; it enforces the uncrossability constraint between α and the PP segment j on the second chain. For an explicit form of \vec{T} [12] we treat the interacting PP steps as colliding needles. The “localized” two-chain evolution operator governing transverse PP motion is

$$\Omega_{loc}^\dagger = -1 + \frac{\bar{r}_l^2}{4} \sum_{n,m=1}^Z (\nabla + \vec{T}(nm)) \cdot (2\vec{I} - \vec{u}_n \vec{u}_n - \vec{u}_m \vec{u}_m) \cdot \nabla. \quad (2)$$

Equation (1) involves Z^2 time-dependent correlations between α and the PP steps on the interpenetrating chain. We invoke two key approximations to make further progress: (i) the off-diagonal (i.e. $j \neq k$) elements in Eq. (1) vanish, and (ii) when evaluating the integral over diagonal elements, the terms in Ω_{loc}^\dagger with $n \neq \alpha, m \neq j$ can also be neglected. These approximations are consistent with our theory for infinitely thin, non-rotating 3D crosses [13], which was favorably compared with simulation [14, 15]. Physically, under quenched-reptation conditions we interpret (i) as neglecting simultaneous ternary and higher-order PP interactions and assuming that on average there are no angular correlations between steps at the PP level.

Approximation (ii) is consistent with idea that under quenched-reptation conditions the chain does not displace enough to change the pair of interacting PP steps over the time scales describing tube localization.

After the above approximations, Eq. (1) involves a sum over Z identical terms. For a given PP step length L_e , each of these terms can be analytically evaluated [9, 11, 13] (for details see Supplemental Material [16]). The textbook picture of PP coarse-graining assumes that L_e (the entanglement length scale) is self-consistently set by the size of the confining tube, i.e., $L_e = \sigma\sqrt{N_e} = A\bar{r}_l$ with $A=2$. Written in terms of the invariant packing length, $p = (N\rho\sigma^2)^{-1} \equiv (\rho_s\sigma)^{-1}$, which quantifies how polymers fill space [17], the evaluation of Eq. (1) with $A=2$ yields

$$\bar{r}_l = \frac{4\sqrt{2}}{A\pi F(A)} p \rightarrow L_e = 2\bar{r}_l = 10.2p, \quad (3)$$

where $F(x)$ is described in the Supplemental Material [16]. The level of quantitative agreement between Eq. (3) and the experimental determination of $d_r \equiv 2\bar{r}_l \approx 17.7p$ in hundreds of flexible chain polymer melts [17] seems remarkable given the simplifying approximations employed. Equation (3) can be viewed as a first-principles derivation of the Lin-Noolandi conjecture for polymer melts, which asserts that a fixed, universal number n of PP segments can fit inside a volume d_r^3 [18, 19]. Our estimate of $n = d_r / p$ is roughly a factor of two smaller than experiment, consistent with the expectation that quenching the rotational PP degree of freedom will overestimate the confining constraints.

Just as in the needle theory, the nonlinear-Langevin-equation (NLE) approach allows one to go beyond the Gaussian analysis and construct the full anharmonic tube-confinement potential [9]. The NLE stochastic equation of motion for the transverse CM displacement (r_{\perp}) of a PP step is $-\zeta_s \frac{dr_{\perp}}{dt} - \frac{\partial}{\partial r_{\perp}} F_{dyn}(r_{\perp}) + \delta f_s = 0$. Here, ζ_s is the short-time (bare) friction constant, δf_s is the corresponding white-noise random force, and $F_{dyn}(r_{\perp})$ is a dynamic confinement potential (in units of $k_B T = 1$) that follows from integrating the displacement-dependent transverse force,

$$f(r_{\perp}) = \frac{-2}{r_{\perp}} + \frac{2}{r_{\perp} F(A)} F\left(\frac{L_e}{r_{\perp}}\right). \quad (4)$$

For rigid needles the NLE extension has been quantitatively compared with experiments on heavily entangled f-actin solutions in the Gaussian and exponential-tail displacement regimes of the confinement potential [20]. For chains we predict that F_{dyn} depends only on the ratio $A = L_e / \bar{r}_l$; Fig. 1 shows confinement potentials for three values of A .

Normalizing $P(r_{\perp}) \sim \exp[-F_{dyn}(r_{\perp})]$ yields the probability distribution of transverse displacements on time scales when the polymer has equilibrated inside the tube but not yet relaxed via reptative motions. Figure 2 presents a comparison between our predicted $P(r_{\perp})$ and the distribution of individual segments from their PP step in an atomistic simulation [21]. The simulations report displacements of individual segments or *beads* relative to the PP step containing the bead, whereas our theory predicts displacements of the PP itself. To perform the comparison we assume the bead displacement distribution can be modeled by taking \bar{r}_l / L_e to be the ratio of the average bead displacement to primitive path length; Table 1 of Ref. [21] implies

$\bar{r}_i / L_e \approx 0.18, 0.22$ for polyethylene and polybutadiene, respectively. The result $A \neq 2$ arises because at the topological PP scale the chain has random walk statistics, but at the network-mesh scale of the beads there are still orientational correlations between consecutive entanglements [21]. This is consistent with recent studies that suggest a factor of ~ 2 difference between “topological” and “rheological” entanglement lengths (the latter determines the plateau modulus) [22]. Accounting for this value of A leads to an accurate transverse confinement potential while only modestly changing the predicted tube diameter, $d_T(A^{-1} = 0.2) = 8.24 p$.

As seen in Fig. 1, the theory is only very weakly sensitive to the difference between $A^{-1} = 0.18, 0.22$, but $A^{-1} \approx 0.5$ and $A^{-1} \approx 0.2$ are quite different. For clarity, in Fig. 2 only results for $A^{-1} = 0.2$ are shown. The agreement between theory and simulation using this value, while imperfect, is striking: the shape of the distribution quite accurate over all length scales, and the exponential tail is very well reproduced. Additionally, the simulations find that when displacement is normalized by $\langle r_{\perp} \rangle$ the distribution is universal, and the theoretical anharmonic confinement potential is similarly universal, up to the very weak dependence on A noted above.

Within the classic tube-model framework the terminal relaxation time is understood by arguing that a PP segment must take $(L/d_T)^2 \propto N/N_e$ diffusive “steps” to exit the tube and allow the mapped chain to fully randomize its orientation, leading to $\tau_{rot} \propto N\tau_{Rouse} / N_e \propto N^3 / N_e$ (where the standard Rouse time has been employed [3]). By invoking a Fickian perspective the CM diffusion constant would be $D \propto L^2 / \tau_{rot} \propto N_e / N^2$. However, it is possible to extend our approach to predict these scaling relations. First, neglecting off-diagonal terms as above, the formal result for the *isotropic* long-time inverse CM diffusion constant (related to the total

friction constant that follows from integrating the force-force time correlation function of the chain) is

$$D_{CM}^{-1} = D_0^{-1} - \frac{\rho}{24\pi^2} \tilde{I} : \int d\vec{v} d\gamma d\vec{r}_{12} \sum_{i,j,k,l=1}^Z \tilde{T}(ij)(\Omega_e^\dagger)^{-1} \tilde{T}(kl) \quad (5)$$

The PP coarse graining renormalizes the local friction constant, so the bare diffusion constant maps to Rouse diffusion of a single PP step of N_e beads, $D_0 \rightarrow D_R = D_{mon} / N_e$, where D_{mon} is the segmental diffusion constant. Equation (5) describes the effective diffusion of an instantaneous conformation of PP steps interacting with other instantaneous conformations of PP steps, subject to the constraint that the conformations neither change nor rotate. Explicitly solving Eq. (5) results in $D_{CM} / D_{mon} \approx N_e^{-1} - 0.54N / N_e^2$. Hence, we predict isotropic motion vanishes when $N \approx 2N_e$.

The geometric complexities of the many connected primitive paths precludes rigorously including anisotropic, reptative-like diffusion. For needles one can decompose the motion into fast longitudinal motion and constrained transverse motion, but for chains longitudinal motions along different PP steps add incoherently in the laboratory frame. However, one can invoke the physically-motivated idea that reptative diffusion is controlled by the *coherent* motion of PP steps due to chain connectivity and compute the renormalized friction constant (from the inverse effective diffusion constant) as an *equally-weighted* sum of the slowly-relaxing terms in Eq. (5). That is, the equivalent of the fast “longitudinal” mode is each PP step moving along its own axis (each term in the sum is thus contracted with the corresponding tensor $(\tilde{I} - \vec{u}_i \vec{u}_i)$ instead of rigorously contracting the entire effective diffusion tensor with a single lab-frame tensor as in Eq. (5)). Finally, we use Szamel’s theory for transverse PP motion [11] as a sensible surrogate

for the rotational relaxation of each diagonal term in Eq. (5). The self-consistent equation for the diffusion constant can then be evaluated as

$$\frac{D_{CM}}{D_0} \approx \left(1 + 9.99 \frac{N}{N_e} \sqrt{\frac{D_0}{D_{CM}}} H \left(\frac{D_{CM}}{D_0} \right) \right)^{-1}, \quad (6)$$

where the function H is defined in Ref. [11]. For $N \gg N_e$ this simplifies considerably: we find

$$D_{CM} / D_R \approx 0.567 N_e / N, \text{ almost exactly the phenomenological result of } D_{CM} / D_R \approx N_e / 3N \text{ [3].}$$

One might expect that a PP step on a tagged polymer likely only interacts with one PP step on another given entangled chain. Thus, to check our interpretation of the physical meaning of the off-diagonal terms discarded above, we consider mapping the chains to a fluid of *disconnected* primitive path segments. This calculation is straightforward: the needle theory [9, 11] is applied to Eq. (1) without the double summation where the PP density replaces the chain density, $\rho_{pp} = Z\rho$, and the T -operators govern the collisions of rods of length L_e . The result is a d_T and effective confinement potential for a given primitive path step *identical* to the Eqs. (3,5). This concurs with the physical intuition that PP-level localization is “aware” of intra-chain connectivity only as a second-order effect on the timescale of interest. In contrast, disconnected PP transverse diffusion proceeds as $D_{\perp} / D_{\perp,0} \approx 18\pi p^2 / L_e^2$ for $N \gg N_e$, a factor of Z^{-2} different from the chain CM diffusion constant obtained above. This incorrect result is expected, since by disconnecting the chain diffusive motion must be massively (and artificially) enhanced.

We now demonstrate that, surprisingly, the results from treating chains as connected primitive-path steps are quite similar to a truly minimalist mapping: replacing *entire* chains by single uncrossable needles. Replacing an entire chain with one degree of freedom is in the spirit

of recent “super coarse-graining” (SCG) methods that substitute a single fictitious particle for entire polymer chains [1]. Soft ellipsoidal particles are able to accurately predict long-time unentangled Rouse dynamics for short chains [23], but modeling interparticle interactions to recover both equilibrium structure and dynamics of long chains is very difficult [1, 24]. Here we investigate whether such a radical reduction in degrees of freedom is able to *predict* from first principles various entanglement phenomena. This approach is known to be sensible for studying the crossover from unentangled to entangled behavior from PP-simulation analyses of the topology-preserving network that defines the melt. Crucially, melts of chains with $N < N_e$ are not entangled and a PP analysis returns a liquid of rigid rods with mean length equal to the average polymer end-to-end distance [25, 26]. In light of this, one would expect a SCG to correctly capture aspects of the entanglement crossover.

Our specific SCG is to identify the needle length with the average long axis of an instantaneous chain conformation, schematically illustrated in the upper cartoon of Fig. 1. Instantaneous polymer conformations are anisotropic; quantifying this anisotropy using simulation data from Ref. [27], a flexible chain is replaced by a needle of length $L \approx \sigma\sqrt{N}/1.3$. The dimensionless coupling constant of the needle theory becomes $\rho L^3 \approx \sigma\sqrt{N}/(1.481p)$. The number of segments in an entanglement strand follows from our prior prediction for the crossover density $\rho_e L^3 \approx 10.1$, defined as the intersection between the independent-binary-collision regime and the asymptotic reptative scaling behavior [9]. This value of the crossover density corresponds to having ~ 10 entangled chains within an end-to-end distance of a given chain, and implies $N_e \approx 244(p/\sigma)^2 = 244\rho_s p^3$, very close to the experimental finding of

$N_e \approx 313\rho_s p^3$ [17]. The PP step length can be independently predicted by using the transverse localization length of the rod CM [9, 11] as a surrogate for the localization of a PP step. The result for $N \gg N_e$ is $L_e = 2r_l = 16\sqrt{2}/(\pi\rho L^2) \approx 9.36p$, very similar to the PP analysis presented above. Remarkably, as shown in Fig. 2, this SCG also results in an accurate tube confinement potential, although here the normalized potential is weakly N/N_e -dependent, in apparent contrast with simulation [21]. The similarities between the two coarse graining schemes hint at a deep connection between the entanglement physics of flexible coils and rigid rods: a universal functional form describes the transverse confinement potential in both systems. This is reminiscent of the finding that PP analyses can provide a way to renormalize “loosely” to “tightly” entangled systems by examining the entanglement plateau modulus [28].

In summary, we have constructed a first-principles microscopic theory for the dynamics of entangled random coil polymers at the primitive-path level, self-consistently renormalizing interchain PP interactions to construct the full anharmonic tube confinement potential. This responds to a major theoretical challenge in understanding highly entangled polymer chain dynamics [5, 6]. The close agreement between the theoretical confining potential and simulation at the PP level suggests a potential application of our work in improving slip-link model simulations by replacing the harmonic springs typically employed to mimic entanglement constraints [29]. Another potential application is a truly microscopic analysis of the entanglement plateau modulus, a long-standing and theoretically difficult issue associated with the relative importance of bonded and non-bonded stresses (or intra- and inter-chain forces) [3, 30–32]. The usual Doi-Edwards assumption is that intrachain terms dominate, but simulations

find that the magnitude of the interchain terms is more compatible with the total contribution to the stress [32]. How these different stress-storage contributions change under deformation could be quite different, and our theory is in a unique position to microscopically evaluate this issue.

Finally, a potential advantage of our microscopic theory is that it provides a tractable conceptual and computational framework to implement specific modifications to the basic reptation-tube model. For instance, the effect of contour length fluctuations can be modeled by keeping the mean value fixed at the equilibrium length but stochastically sampling PP step lengths (or SCG mapped needle lengths) from a Gaussian distribution. Our prediction of anharmonic transverse confinement may have major implications for how the tube model is modified under nonlinear rheological deformations, where the question of how large deformations soften, or even destroy, the confining tube is a frontier issue [33 – 37]. We recently studied such effects for large-amplitude step-strains of entangled needle fluids [38], and plan to soon extend the calculation to entangled chains.

Acknowledgments. We thank Christos Tzoumanekas and Doros Theodorou for sending the chain simulation data, and Grzegorz Szamel for valuable correspondence and comments on this manuscript. This work was supported by the Nanoscale Science and Engineering Initiative of the National Science Foundation under NSF Award DMR-0642573.

References

- [1] J. T. Padding and W. J. Briels, *J. Phys.: Condens. Matter* **23**, 233101 (2011); A. A. Louis, P. G. Bolhuis, J. P. Hansen and E. J. Meijer, *Phys. Rev. Lett.* **85**, 2522 (2000).
- [2] P. G. de Gennes, *J. Chem. Phys.* **55** 572 (1971)
- [3] M. Doi and S. F. Edwards, *The Theory of Polymer Dynamics*, (Oxford University Press, Oxford, UK, 1986)
- [4] T. C. B. McLeish, *Adv. Phys.* **51**, 1379 (2002).
- [5] A. E. Likhtman, *J. Non-Newtonian Fluid Mech.* **157**, 158 (2009).
- [6] R. G. Larson, *J. Poly. Sci. B: Poly. Phys.* **45**, 3240 (2007).
- [7] R. Everaers, et. al., *Science* **303**, 823 (2004).
- [8] Q. Zhou and R. G. Larson, *Macromolecules* **39**, 6737 (2006).
- [9] D. M. Sussman and K. S. Schweizer, *Phys. Rev. Lett.* **107**, 078102 (2011).
- [10] G. Szamel, *Phys. Rev. Lett.* **70**, 3744 (1993).
- [11] G. Szamel and K. S. Schweizer, *J. Chem. Phys.* **100**, 3127 (1994).
- [12] B. Cichocki, *Z. Phys. B – Condens. Mat.* **66**, 537 (1987).
- [13] D. M. Sussman and K. S. Schweizer, *Phys. Rev. E* **83**, 061501 (2011).
- [14] W. van Ketel, C. Das, and D. Frenkel, *Phys. Rev. Lett.* **94**, 135703 (2005).
- [15] P. Charbonneau, C. Das, and D. Frenkel, *Phys. Rev. E* **78**, 011505 (2008).
- [16] See Supplemental Material at (APS web link to be inserted)
- [17] L. J. Fetters, D. J. Lohse, D. Richter, T. A. Witten, and A. Zirkel, *Macromolecules*, **27**, 4639 (1994).
- [18] Y.-H. Lin, *Macromolecules* **20**, 3080 (1987).
- [19] T. A. Kavassalis and J. Noolandi, *Phys. Rev. Lett.* **59**, 2674 (1987).
- [20] B. Wang, et. al., *Phys. Rev. Lett.* **104**, 118301 (2010).
- [21] C. Tzoumanekas and D. N. Theodorou, *Macromolecules* **39**, 4592 (2006).

- [22] R. Everaers, Phys. Rev. E **86**, 022801 (2012).
- [23] M. Murat and K. Kremer, J. Chem. Phys. **108**, 4340 (1998).
- [24] I. Y. Lyubimov, J. McCarty, A. Clark, and M. G. Guenza, J. Chem. Phys. **132**, 224903 (2010).
- [25] S. Shanbhag and R. G. Larson, Macromolecules **39**, 2413 (2006).
- [26] C. Tzoumanekas, F. Lahmar, B. Rousseau, and D. N. Theodorou, Macromolecules **42**, 7474 (2009).
- [27] T. D. Hahn, E. T. Ryan, and J. Kovac, Macromolecules **24**, 1205 (1991).
- [28] N. Uchida, G. S. Grest, and R. Everaers, J. Chem. Phys. **128**, 044902 (2008).
- [29] V. C. Chappa, D. C. Morse, A. Zippelius, and M. Müller, Phys. Rev. Lett. (in press)
- [30] M. Fixman, J. Chem. Phys. **95**, 1410 (1991).
- [31] J. Gao and J. H. Weiner, Science **266**, 748 (1994).
- [32] J. Ramirez, S. K. Sukumaran, and A. E. Likhtman, J. Chem. Phys. **126**, 244904 (2007).
- [33] D. M. Sussman and K. S. Schweizer, J. Chem. Phys. **135**, 131104 (2011).
- [34] S. Q. Wang, S. Ravindranath, Y. Wang, and P. Boukany, J. Chem. Phys. **127**, 064903 (2007).
- [35] P. E. Boukany, S. Q. Wang, and X. Wang, Macromolecules **42**, 6261 (2009).
- [36] A. Kushwaha and E. S. G. Shaqfeh, J. Rheol. **55**, 463 (2011).
- [37] C. Baig, V. G. Mavrantzas, and M. Kröger, Macromolecules **43**, 6886 (2010).
- [38] D. M. Sussman and K. S. Schweizer, Macromolecules **45**, 3270 (2012).

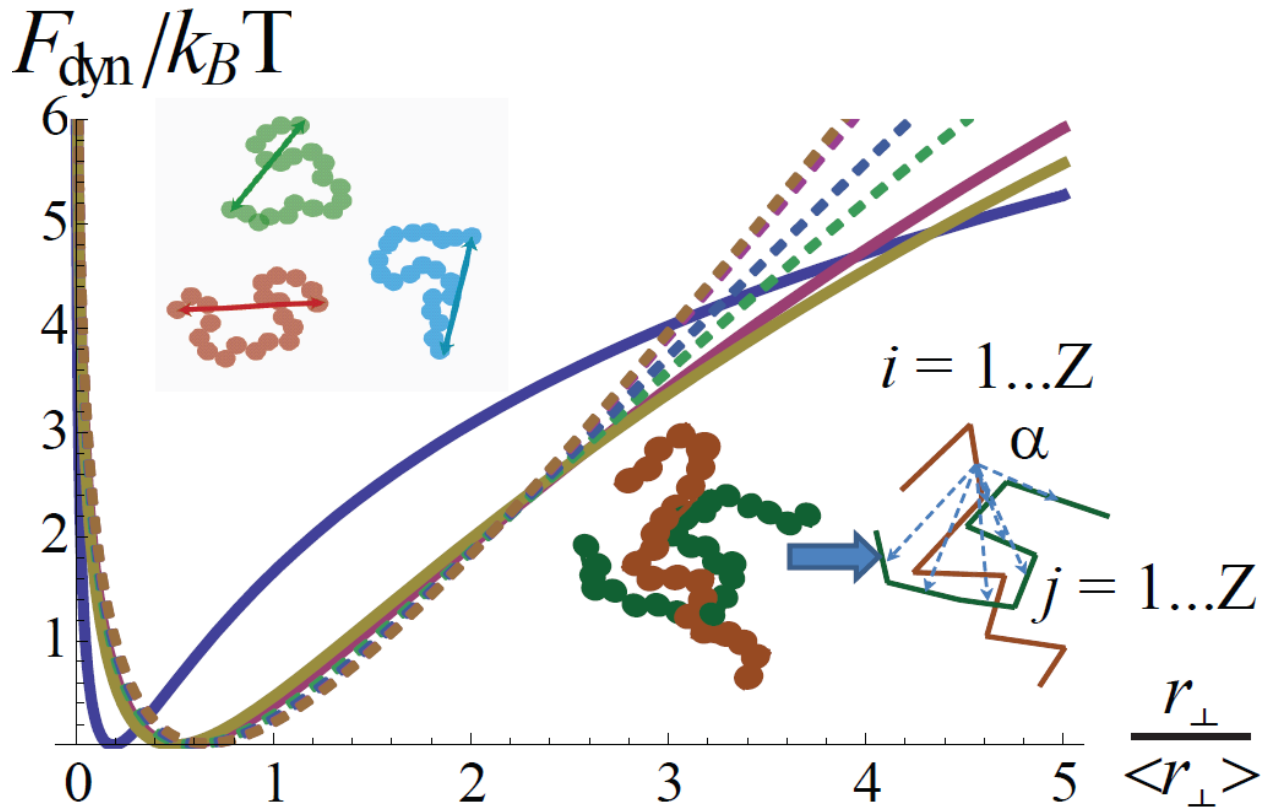


Figure 1. Transverse confinement potential for the PP mapping as a function of normalized transverse displacement (solid curves, $A^{-1} = 0.5, 0.22, 0.18$, left to right) and for the SCG needle limit with $N/N_e = 10, 20, 100, 200$ (dashed curves, bottom to top). Cartoons below and above schematically depict the two mappings.

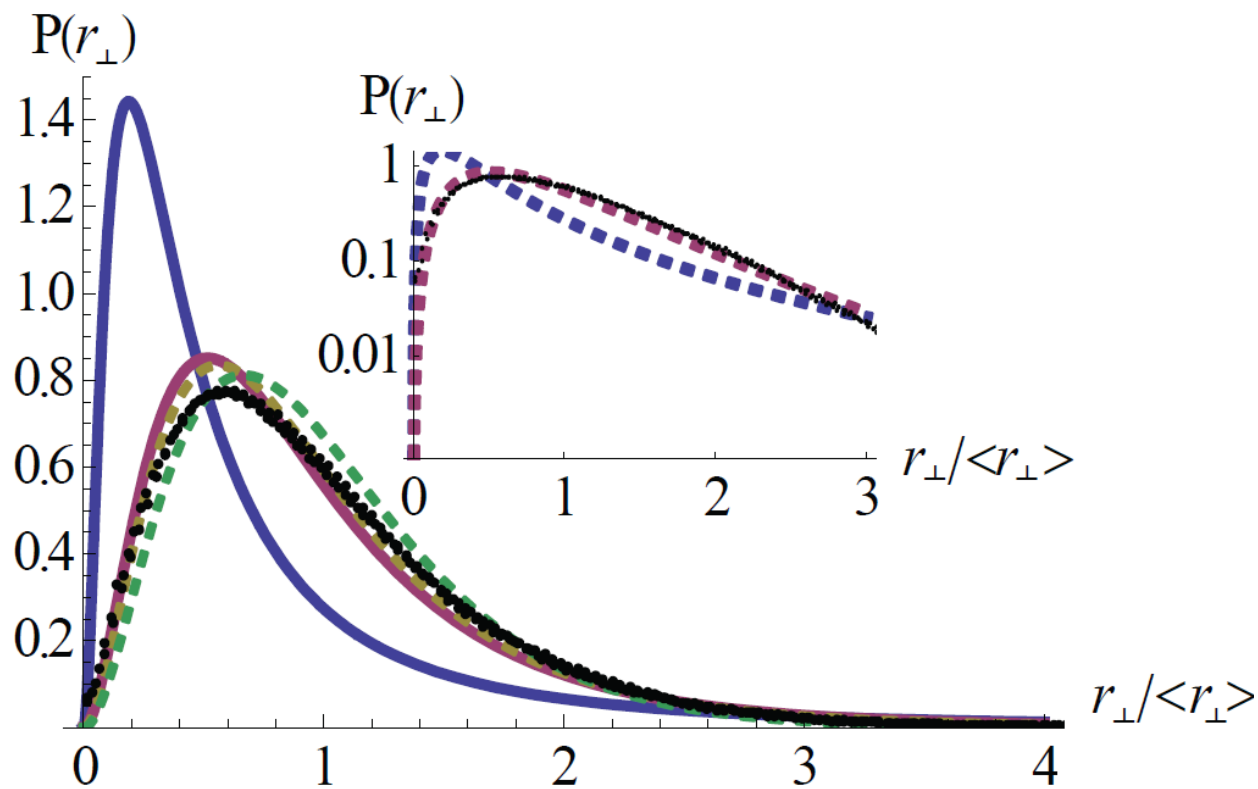


Figure 2. Transverse-displacement probability distribution compared with simulation [20] (points). Solid curves are theoretical predictions with $A^{-1} = 0.5, 0.2$ (left and right); dashed curves are the chain-to-needle mapping results for $N / N_e = 6, 18000$ (left and right). Inset: Log plot of PP distribution with $A^{-1} = 0.5, 0.2$ compared with simulation.